

## Cool-Core Cycles and Phoenix

DEOVRAT PRASAD,<sup>1</sup> PRATEEK SHARMA,<sup>2,3</sup> ARIF BABUL,<sup>4</sup> G. MARK VOIT,<sup>1</sup> AND BRIAN W. O'SHEA<sup>1,5</sup>

<sup>1</sup>*Department of Physics and Astronomy, Michigan State University, MI, US*

<sup>2</sup>*Department of Physics, Indian Institute of Science, Bangalore, India*

<sup>3</sup>*Max-Planck Institute of Astrophysics, Garching, Germany*

<sup>4</sup>*Physics and Astronomy, University of Victoria, Victoria, Canada*

<sup>5</sup>*Department of Computational Mathematics, Science, and Engineering, Michigan State University, MI, US*

### ABSTRACT

Recent observations show that the star formation rate (SFR) in the *Phoenix* cluster is  $\sim 500 M_{\odot} \text{ yr}^{-1}$ . Even though *Phoenix* is a massive cluster,  $M_{200} \approx 1.8 \times 10^{15} M_{\odot}$ , such a high SFR is not expected in a scenario in which feedback from an active galactic nuclei (AGN) maintains the intra-cluster medium (ICM) in a state of rough thermal balance. It has been argued that either AGN feedback saturates in massive clusters or the central super massive black hole (SMBH) is small compared to what is needed for efficient kinetic feedback and hence unable to quench the catastrophic cooling. In this work, we present an alternate scenario wherein intense short-lived cooling and star formation phases are part of the AGN feedback loop – the cool core cooling and heating cycles. Using results from our 3D hydrodynamic simulation of a standard cool-core cluster ( $M_{200} \sim 7 \times 10^{14} M_{\odot}$ ), we argue that *Phoenix* is in a cooling state in which an AGN outburst has just started and has not yet arrested core cooling. This state of high cooling rate and star formation is expected to last only for  $\lesssim 100$  Myr in *Phoenix*.

*Keywords:* Galaxy Clusters, Cooling flow, Black Hole, AGN feedback, Intra-cluster medium

### 1. INTRODUCTION

Recent deep multi-wavelength observations of the *Phoenix* cluster by McDonald et al. (2014, 2019a,b) have detected a star formation rate of  $\sim 500 M_{\odot} \text{ yr}^{-1}$  ( $z \approx 0.6$ ) in the cluster core ( $r < 50$  kpc). In the standard AGN feedback scenario such a high star formation rate is not expected even in the case of a massive galaxy cluster like *Phoenix* ( $M_{200} \approx 3 \times 10^{15} M_{\odot}$ ). Such a high star formation rate, which is being attributed solely to cooling of the intra-cluster medium (ICM), is expected for a pure cooling flow in the absence of heating. This is unlike another massive galaxy cluster, CL09104, where a high star formation rate ( $70 - 200 M_{\odot} \text{ yr}^{-1}$ ) is due to an ongoing merger (O'Sullivan et al. 2012). Given that the cooling time,  $t_{\text{cool}} \equiv 3nk_{BT}/[2n_e n_i \Lambda]$ , in the central  $r < 20$  kpc is an order of magnitude shorter than in any other observed galaxy cluster, it is being speculated that *Phoenix* has experienced a different evolutionary pathway than normal cool-core clusters (McDonald et al. 2019a).

For *Phoenix*, the ratio of the cooling time and the free-fall time ( $t_{\text{ff}} \equiv [2r/g]^{1/2}$ ) reaches  $\sim 1$  at  $r \approx 3$  kpc (McDonald et al. 2019a). The intra-cluster medium (ICM) is expected to become multiphase, leading to star formation and AGN outbursts whenever  $\min(t_{\text{cool}}/t_{\text{ff}}) \lesssim 10$  (McCourt et al. 2012; Sharma et al. 2012b). Most cool core clusters are observed to be in a state of rough thermal balance with  $\min(t_{\text{cool}}/t_{\text{ff}})$  between 10 – 20 (Voit et al. 2015b,a; Hogan et al. 2017; Pulido et al. 2018), with a very few clusters below 10 and none below 5. *Phoenix* is the first observed galaxy cluster to have  $\min(t_{\text{cool}}/t_{\text{ff}}) \sim 1$  in the ambient medium, making it an outlier from standard cool cores.

*Phoenix* shows large intrinsic X-ray luminosity ( $\approx 4.7 \times 10^{45} \text{ erg s}^{-1}$ ; Ueda et al. 2013). The cavity power is  $10^{46} \text{ erg s}^{-1}$  assuming the AGN has shut off and cavities are rising buoyantly (Russell et al. 2017; McDonald et al. 2019a). With the measured cavity power small compared to the halo mass, it is being argued that the mechanical jet power has saturated and is unable to quench the cooling flow in a massive galaxy cluster signalling the failure of kinetic SMBH feedback (McDonald et al. 2019a).

In this work, we argue that *Phoenix* is not fundamentally different from other cool-core clusters – by chance we have caught it in a short lived cooling state (with AGN feedback just turning on). It also does not necessarily signal the failure of kinetic SMBH feedback. Such phases are seen in simulations of halos across a range of masses (Prasad et al. 2015; Li et al. 2015; Prasad et al. 2018), albeit the cooling phases are more frequent in more massive halos for a fixed accretion efficiency parameter. This is because even strong feedback is unable to push gas much farther in a more massive halo. Using the 3D hydrodynamic NFW+BCG simulation without stellar depletion (fiducial run) in Prasad et al. (2018), we present an alternate scenario in which *Phoenix* is in a state of early AGN outburst following the cooling phase in the core of a cluster. This transitional phase is expected to last for only  $\sim 50 - 100$  Myr, after which the AGN will heat and disperse the core to a state similar to other cool cores.

## 2. COOLING AND INITIAL AGN HEATING PHASE

In the simulation discussed here, the intra-cluster medium is initialised in hydrostatic equilibrium in the gravitational potential given by the sum of a Navarro-Frenk-White (NFW) potential for the dark matter halo and a singular isothermal sphere (SIS) potential for the central brightest cluster galaxy (BCG). The initial  $\min(t_{\text{cool}}/t_{\text{ff}})$  for the fiducial run is  $\approx 7$  at  $r \approx 10$  kpc and the cooling time is  $\approx 200$  Myr in the core. Accretion rate ( $\dot{M}_{\text{acc}}$ ) is calculated at 0.5 kpc and bipolar kinetic feedback jets with power  $\epsilon \dot{M}_{\text{acc}} c^2$  are injected at small radii (for details see Prasad et al. 2015, 2018). As the galaxy cluster is initialized in hydrostatic equilibrium, initially there is negligible accretion ( $\dot{M}_{\text{acc}}$ ), and therefore there is no jet injection. After a core cooling time ( $\approx 200$  Myr) the cooling-flow accretion rate ( $\dot{M}_{\text{acc}}$ ) rises, resulting in enhanced AGN jet power. The AGN jet outburst heats the core, pushes gas around, and raises  $t_{\text{cool}}/t_{\text{ff}}$ , keeping the average  $\dot{M}_{\text{acc}}$  well below the cooling flow value. The cool core undergoes multiple radiative cooling and AGN heating cycles throughout its lifetime.

Figure 1 shows the density (upper panels) and temperature (lower panels) slices during a cooling phase at  $t = 1.93$  Gyr (left panels) and the subsequent AGN outburst phase at  $t = 1.95$  Gyr (right panels). These epochs correspond to a strong starburst phase before AGN feedback couples to the ICM and quenches star formation (see the right panel in Fig. 4 of Prasad et al. 2018).

Figure 2 shows the projected surface brightness maps of the X-ray gas (0.5-10 keV) in the cluster core at the same two times as Figure 1. During the cooling phase the surface brightness is almost uniform within  $r \sim 10$

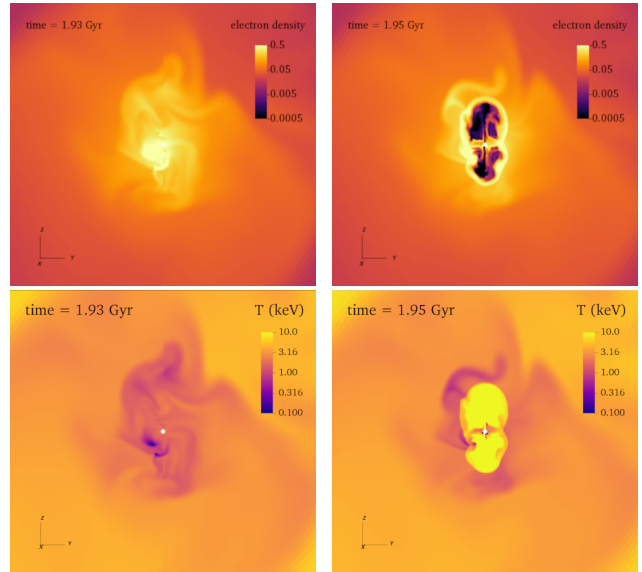


**Figure 1.** Electron number density ( $n_e$ ) in  $\text{cm}^{-3}$  (upper panels) and temperature ( $T$ ) in keV (lower panels) in  $60 \text{ kpc} \times 60 \text{ kpc}$  slices within the plane of jet injection. Two epochs are shown, one near the end of the cooling phase (at 1.93 Gyr, left panels) and the other at the beginning of the AGN outburst phase (at 1.95 Gyr, right panels). The cooling phase exhibits filamentary structures condensing out in the core ( $r \lesssim 25$  kpc). During the initial AGN outburst phase high density shocked regions are seen around the cavities inflated by AGN jets.

kpc. The morphology is then altered as AGN jets make their way out of the core. The later surface brightness maps shows sharp peaks in the shocked regions around the AGN cavity in the right panel.

Morphologically, *Phoenix* appears to be in a state similar to our  $t = 1.95$  Gyr snapshots (compare our Figs. 1 & 2 with Figs. 1, 2, and 5 in McDonald et al. 2019a). Current star formation, as traced by UV and [OII], appears enhanced at the periphery of the X-ray cavity created by the AGN outburst. The bipolar X-ray cavities observed in *Phoenix* are attached to the center and have a major axis of  $\sim 25$  kpc, rather similar to, but somewhat bigger than, in our simulations at 1.95 Gyr.

Cooling and nascent AGN phases are expected to be more frequent in more massive halos for a fixed accretion efficiency because of the deeper potential well (for details, see Section 3.2.2 in Prasad et al. 2015). This suggests that the likelihood of observing a massive halo in a cooling state is much higher than that of a lower mass halo. This is probably the reason why the first detection of a galaxy cluster in a cooling phase happens to be a massive cluster. The nature of the cooling and AGN recovery phases appears to be similar across halo masses (see Fig. 12 in Prasad et al. 2015), and with

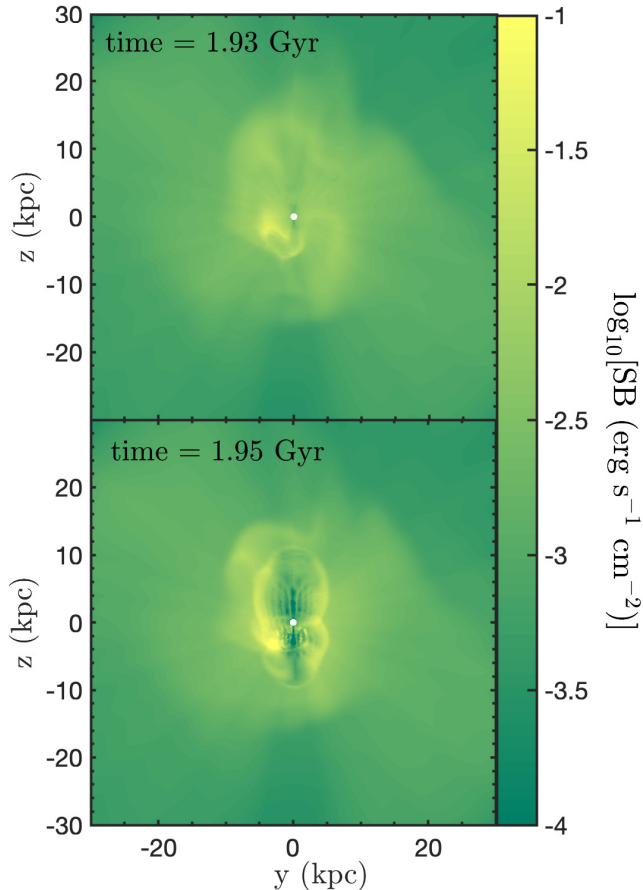


**Figure 2.** X-ray (0.5 – 10 keV) surface brightness maps (projected perpendicular to jet injection) corresponding to the cooling phase at  $t = 1.93$  Gyr (upper panel) and the beginning of AGN outburst phase at  $t = 1.95$  Gyr (lower panel). Cooling phase shows a high X-ray surface brightness in the central ( $r \sim 10$  kpc) regions with an elevated surface brightness extending well beyond 30 kpc. Notice the sharp jump in surface brightness due to the shocked gas around the cavity inflated by jets.

deeper and higher resolution observations we expect to discover *Phoenix*-like phases (with  $\min[t_{\text{cool}}/t_{\text{ff}}] \sim 1$ ) in lower mass clusters and groups.

### 3. THERMODYNAMIC PROFILES

*Phoenix* shows unique entropy, cooling time, and  $t_{\text{cool}}/t_{\text{ff}}$  profiles in the core ( $r < 50$  kpc) compared to any other observed cluster. However, a comparison of the *Phoenix* cluster thermodynamic profiles with the cooling and initial AGN outburst phase of our fiducial run shows close similarities. The top left panel in Figure 3 shows the azimuthally-averaged emissivity weighted entropy profile of X-ray gas (0.5-10 keV) during the cooling (solid lines) and initial AGN outburst phases (dot-dashed lines) for our fiducial run. Plots show that

the entropy during the cooling phase in the central 10 kpc region falls below  $10 \text{ keV cm}^2$  and remains below this value even 20 Myr after the onset of AGN feedback as the jets drill their way out of the core. The observed entropy profile (solid black line with circles) in *Phoenix* shows a similar behaviour. Similarly, the cooling time (bottom left panel) in the central 10 kpc falls to 10s of Myr during the intense cooling phase. The cooling time remains below 100 Myr in the core ( $r < 10$  kpc) during the early stages of the AGN outburst phase. This is also similar to the cooling time profile observed in *Phoenix* (solid black line with circles). The  $T_{\text{keV}}/T_{\text{vir}}$  plot with radius (top right panel, Figure 3) shows that the dip in the temperature profile for *Phoenix* in the central  $r < 20$  kpc is consistent with the cooling phase of a cool core cluster. Also note that the observationally derived density profiles are expected to be biased high due to the presence of multiphase gas.

The bottom right panel in Figure 3 shows the cooling time to free-fall time ratio,  $t_{\text{cool}}/t_{\text{ff}}$ , for the fiducial run for a *Phoenix*-like phase. One sees a steady power-law drop down to  $r \lesssim 5$  kpc during the cooling and the early phase of AGN activity with a minimum value of  $\lesssim 5$ . The monotonic drop in  $t_{\text{cool}}/t_{\text{ff}}$  with decreasing radius is similar to *Phoenix*. Even though the minimum cooling time,  $t_{\text{cool}}$ , is a factor of 2 shorter for *Phoenix*,  $t_{\text{cool}}/t_{\text{ff}}$  is very similar at  $r > 5$  kpc.

Figure 4 shows the variation of the  $t_{\text{cool}}/t_{\text{ff}}$  profile for a duration of 150 Myr during a cooling and AGN outburst phase ( $t = 1.85 - 2.0$  Gyr). The color of the lines represents the time as shown in the colour bar. During the initial cooling phase  $t_{\text{cool}}/t_{\text{ff}}$  starts to dip in the central  $r < 30$  kpc and the plasma becomes thermally unstable. Cold gas clumps condense out from the hot ICM, raising the core density and fueling a strong AGN outburst. These profiles show the first signs of AGN heating at 1.94 Gyr within  $r < 3$  kpc. At 1.95 Gyr the effect of AGN heating can be seen extending to  $r < 6$  kpc, although  $\min(t_{\text{cool}}/t_{\text{ff}})$  is still  $\approx 3$ . By 1.96 Gyr, the AGN outburst has driven the core to  $\min(t_{\text{cool}}/t_{\text{ff}}) \approx 5$ , and has driven it to  $\approx 10$  by 2 Gyr. The figure shows that the steady drop in  $t_{\text{cool}}/t_{\text{ff}}$  is maintained for the first  $\approx 20$  Myr of the active AGN phase. During the cooling phase, the cooling rate in the central 10 kpc is  $\sim 200 M_{\odot} \text{ yr}^{-1}$  (about a third of the steady cooling flow rate), leading to accumulation of  $\gtrsim 5 \times 10^9 M_{\odot}$  of cold gas ( $T < 10^4$  K) by 1.95 Gyr. The cooling rate dies down after this as the jets heat up the core, partly evaporating the cold gas leading to a slight decrease in the total cold gas. A similar behaviour is seen for the cooling cycle around  $t = 2.55 - 2.7$  Gyr (see Fig. 3, the right panel of Fig. 4 in Prasad et al. 2018).

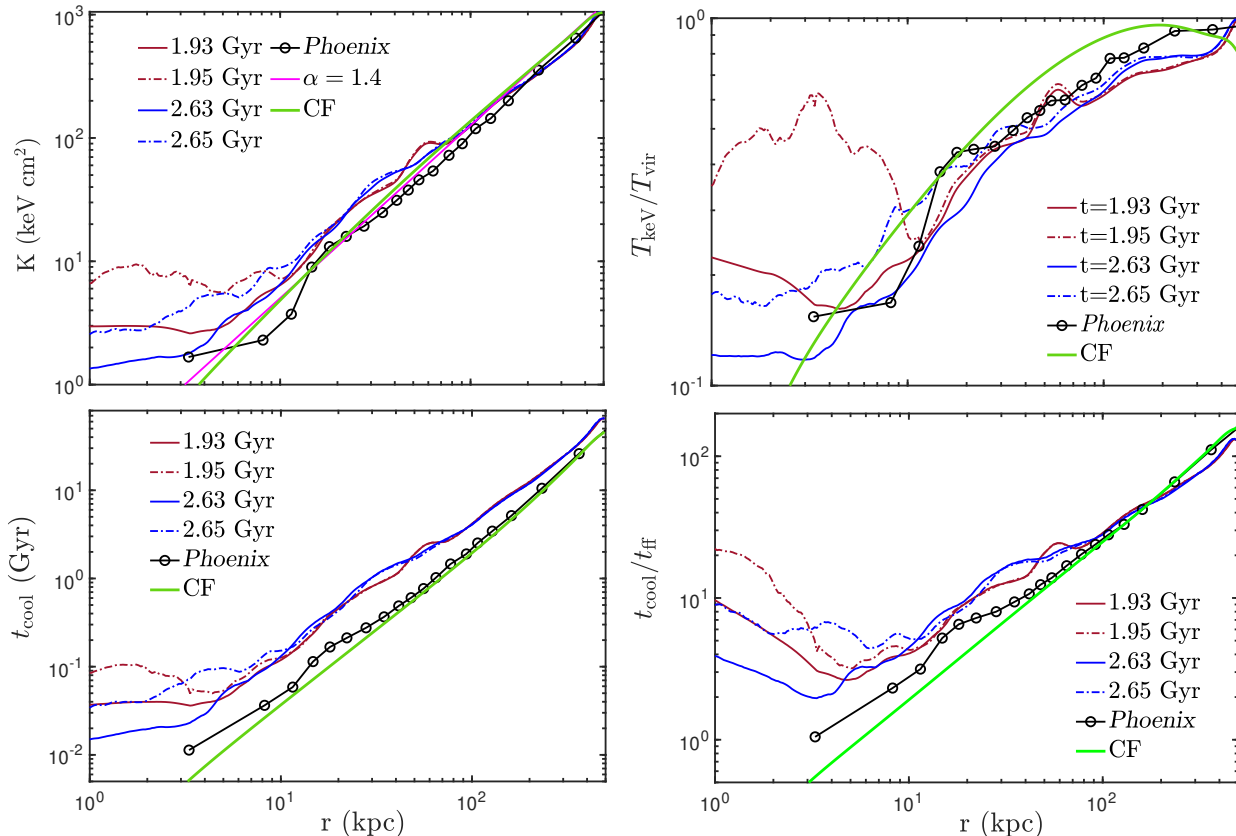


**Figure 3.** Angle-averaged emissivity-weighted (for 0.5 – 10 keV) entropy (top left panel),  $T/T_{\text{vir}}$  (top right panel,  $T_{\text{vir}} = 8.5$  keV for our simulation and 14 keV for Phoenix), cooling time (lower left panel) and  $t_{\text{cool}}/t_{\text{ff}}$  (lower right panel) radial profiles during the cooling phases ( $t = 1.93, 2.63$  Gyr) and the initial jet outburst phases ( $t = 1.95, 2.65$  Gyr) for our fiducial run. During the short-lived (20-50 Myr) cooling phase, the cooling time ( $t_{\text{cool}}$ ) drops to less than 100 Myr in the central 10 kpc causing  $t_{\text{cool}}/t_{\text{ff}}$  ratio to fall below 5 within 5 kpc radius from the center. The cooling phase entropy in the central 10 kpc also falls below 10 keV cm<sup>2</sup>. This behaviour is similar to the observed  $t_{\text{cool}}$ ,  $t_{\text{cool}}/t_{\text{ff}}$  and entropy profiles in the *Phoenix* cluster (solid black line with circles) by McDonald et al. 2019a. The green solid lines show a steady cooling flow solution for a mass-model of Phoenix read-off from Figs. 10 & 11 in McDonald et al. (2019a). Exact comparison with observational profiles is difficult because of a different cluster mass in the simulation and systematic biases introduced by multiphase gas and deprojection in a non-spherically symmetric atmosphere.

Figure 3 also shows (green solid lines) various profiles for a steady cooling flow applied to the mass model of *Phoenix* ( $M_{200} = 2.5 \times 10^{15} M_{\odot}$ ,  $c_{200} = 10$ ,  $V_c = 250$  km s<sup>-1</sup>) and appropriate boundary conditions at 500 kpc ( $n_e = 10^{-3}$  cm<sup>-3</sup>,  $K = 1057$  keV cm<sup>2</sup>). The steady cooling flow model matches the observed profiles (McDonald et al. 2019a; see also Stern et al. 2019) but so do the profiles from our simulations with feedback in the cooling phase. Thus, a match with the cooling flow solution does not necessarily imply an absence of feedback heating. Note that  $t_{\text{cool}}$  in our simulations (which use a lower halo mass; bottom left panel) is longer than in *Phoenix* because a cool-core in lower mass halo is less dense than a more massive halo (Sharma et al. 2012a).

#### 4. NEED FOR DEEPER OBSERVATIONS

Observations of cool core clusters show very few clusters with  $\min(t_{\text{cool}}/t_{\text{ff}})$  in the range 1 – 10. However, the distribution of  $\min(t_{\text{cool}}/t_{\text{ff}})$  from our simulations shown in Figure 11 of Prasad et al. (2018) suggests that systems with  $\min(t_{\text{cool}}/t_{\text{ff}}) \lesssim 5$  should be present. The discovery that the *Phoenix* core has  $\min(t_{\text{cool}}/t_{\text{ff}}) \sim 1$  hints that the observations may be missing such clusters with  $\min(t_{\text{cool}}/t_{\text{ff}}) \lesssim 5^1$  because such states are short lived (see Fig. 4) and the smallest values of  $t_{\text{cool}}/t_{\text{ff}}$  occur at  $\lesssim 10$  kpc, a region unresolved by observations of most cluster cores. The importance of deeper observations is illustrated by the fact that the earlier pro-

<sup>1</sup> The core has to pass through  $\min(t_{\text{cool}}/t_{\text{ff}}) \approx 5$  if it has to end up with  $\min(t_{\text{cool}}/t_{\text{ff}}) \approx 1$ !



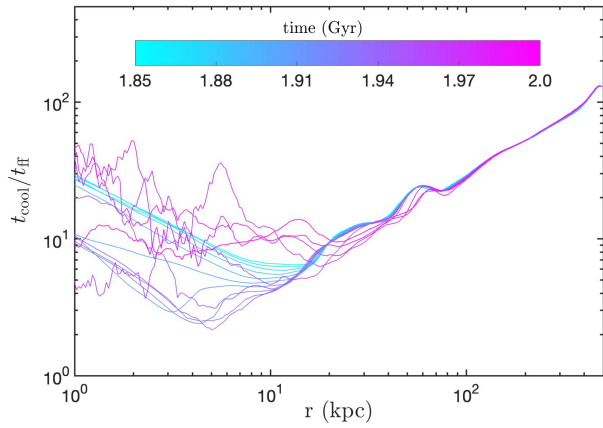


**Figure 4.** Angled-averaged emissivity-weighted (for 0.5–10 keV)  $t_{\text{cool}}/t_{\text{ff}}$  radial profiles of the X-ray emitting gas (0.5–10 keV) from 1.85–2.0 Gyr for our fiducial run. The colours of the lines represent time as shown in the colour bar. The plot shows the variation in  $t_{\text{cool}}/t_{\text{ff}}$  over 150 Myr as the cluster goes through intense cooling and rapid AGN heating phases.

files for *Phoenix* estimate the core temperature to be  $\approx 7$  keV and the core entropy to be  $> 10$  keV cm<sup>2</sup> (see Phoenix [SPT-CLJ2344-4243] in Figs. 3, 5 of McDonald et al. 2019b), significantly higher than the values obtained in the very center by most recent observations (see Fig. 3). The higher photon count in McDonald et al. (2019a) within  $r < 10$  kpc allowed accurate removal of the AGN X-ray point source, revealing sharply peaked diffuse emission indicative of unusually low entropy gas.

Figure 5 tries to quantify the effect of spatial resolution on the estimate of  $\min(t_{\text{cool}}/t_{\text{ff}})$  from X-ray observations. It shows  $\min(t_{\text{cool}}/t_{\text{ff}})$  in our fiducial simulation with time for different inner cut-off radii. The dot-dashed magenta line shows  $\min(t_{\text{cool}}/t_{\text{ff}})$  for  $r > 10$  kpc, the dashed black line for  $r > 5$  kpc and the solid orange line for  $r > 0.5$  kpc. An inner radial cut-off makes the dips in  $\min(t_{\text{cool}}/t_{\text{ff}})$  more pronounced even though the peaks remain unchanged. This is because during the cooling phase the  $t_{\text{cool}}/t_{\text{ff}}$  profile shows a roughly power-law behaviour even within  $r < 5$  kpc, unlike the heating phase in which the minimum is achieved at  $r \gtrsim 10$  kpc (see Fig. 4). Observations with high angular resolution and higher photon count are thus needed for clusters in the cooling phase to accurately extract  $\min(t_{\text{cool}}/t_{\text{ff}})$ . Since a large fraction of observations lack sufficient sufficient photons in the central 10 kpc even for cool cores, observations are expected to overestimate  $\min(t_{\text{cool}}/t_{\text{ff}})$  for the coolest clusters, except perhaps for

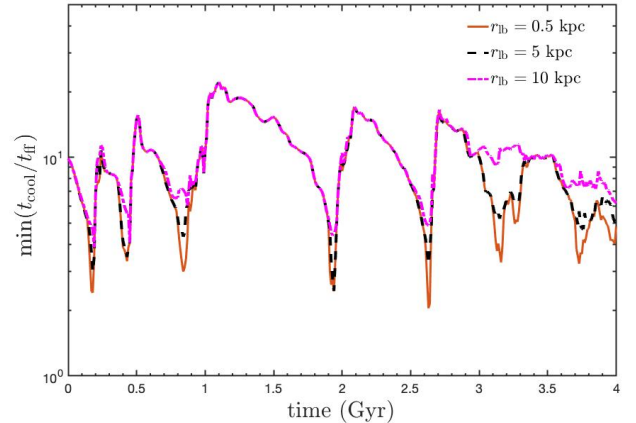


**Figure 5.** The variation of  $\min(t_{\text{cool}}/t_{\text{ff}})$  with time for different inner cut-off radius for our fiducial run. This plot shows the importance of high spatial resolution to obtain the correct value of  $\min(t_{\text{cool}}/t_{\text{ff}})$  in cool core clusters. This important parameter is grossly overestimated if the spatial resolution is  $\gtrsim 10$  kpc.

the very nearby ones. This may largely explain the apparent discrepancy between the observed distribution of  $\min(t_{\text{cool}}/t_{\text{ff}})$  and the distribution obtained from our (and other similar) feedback jet-ICM simulations. Some of the deeper observations like Babyk et al. 2018 do find  $t_{\text{cool}}/t_{\text{ff}} \approx 5$  in some lower mass halos like elliptical galaxies.

## 5. DISCUSSION

We find that unique features of the core of the *Phoenix* cluster are consistent with the kinetic AGN feedback model. They do not necessarily signal a different evolutionary pattern for *Phoenix*, but rather motivate high spatial resolution observations of the most centrally peaked systems to assess if the observed distribution of  $\min(t_{\text{cool}}/t_{\text{ff}})$  is compatible with the simulations.

*Phoenix* shows a high recent SFR but a much smaller fraction of young stars. The massive amount of molecular gas ( $M_{\text{cold}} > 10^{10} M_{\odot}$ ) most likely has originated in gas cooling from the surrounding hot atmosphere over 50 – 120 Myr (Russell et al. 2017). Pure cooling for few 100 Myr (Figure 4) is enough to make the cluster look like a pure cooling flow. This is consistent with our interpretation of a short cooling cycle. Moreover, pure cooling in *Phoenix* for  $\sim 1$  Gyr will create a cold gas reservoir of  $10^{12} M_{\odot}$ , more than an order of magnitude larger than what is observed (Russell et al. 2017).

Another point of contention is the mass of the super massive black hole at the center of *Phoenix*. McDonald et al. 2019a makes a case for a smaller SMBH mass for

the halo mass. McDonald et al. 2012, using the scaling relations between the spheroid stellar mass and the black hole mass (Bennert et al. 2011), determine the SMBH mass  $\sim 1.8 \times 10^{10} M_{\odot}$ . At  $1.8 \times 10^{10} M_{\odot}$ , *Phoenix* hosts one of the most massive SMBHs observed in the universe. Owing to a large Eddington accretion rate, such a massive SMBH can support kinetic feedback even for a large accretion rate. The smaller cavity power observed in *Phoenix* is consistent with the hypothesis that the AGN is in the initial stages of an outburst and suggest an alternative to the scenario proposed in McDonald et al. 2019a that the AGN jet has reached a saturation state and is unable to overcome cooling.

A simple estimate of the expected Phoenix-like systems in the existing X-ray cluster samples such as ACCEPT (Cavagnolo et al. 2009) can be made. There are about 60 clusters with temperature,  $T > 8$  keV in this sample. Assuming a Phoenix-like cooling event every Gyr (see the right panel of Fig. 4 in Prasad et al. 2018), we can expect Phoenix-like phenomena in up to 10% of cool core clusters. If we take a third of these ACCEPT clusters to be cool cores, we expect about two *Phoenix*-like systems. Note that this is a crude estimate based on idealized simulations that do not include cosmological mergers. Mergers may lower the incidence of *Phoenix*-like states but nevertheless, we do expect to see some cool-core clusters populating  $\min(t_{\text{cool}}/t_{\text{ff}}) < 10$  space (see Figure 11 of Prasad et al. (2018)).

## 6. CONCLUSIONS

- Surface brightness snapshots, density, entropy, temperature, and  $t_{\text{cool}}/t_{\text{ff}}$  profiles from our cluster simulations near the end of the cooling phase and beginning of the AGN event are similar to *Phoenix* (although the halo mass of the simulated cluster is a factor of few smaller than Phoenix).
- *Phoenix* is not fundamentally different from other cool-core clusters. We have just caught it in a cooling state (with feedback just turning on).
- *Phoenix* does not necessarily signal the failure of kinetic SMBH feedback. Similar phases may also be seen in lower mass halos, albeit the cooling phases are more frequent in more massive halos for a fixed efficiency parameter.
- Deeper observations with higher photon count within  $r < 10$  kpc of centrally peaked galaxy clusters are required for measuring the  $\min(t_{\text{cool}}/t_{\text{ff}})$  accurately as  $t_{\text{cool}}/t_{\text{ff}}$  during the cooling phase show single power law behaviour well within  $r < 10$  kpc.

DP is supported by *Chandra* theory grant no. TM8-19006X (G. M. Voit as PI) and NSF grant no. AST-1517908 (B.W.O'Shea as PI). BWO acknowledges further support from NASA ATP grant NNX15AP39G. A.B. acknowledges support from NSERC through the Discovery Grant program. P.S. acknowledges a Swarnajayanti Fellowship from the Department of Science and Technology, India (DST/SJF/PSA-03/2016-17) and thanks the Humboldt Foundation for support that enabled his sabbatical at MPA. We thank Michael McDonald for useful discussions.

## REFERENCES

- Babyk, I. V., McNamara, B. R., Nulsen, P. E. J., et al. 2018, ApJ, 862, 39
- Bennert, V. N., Auger, M. W., Treu, T., Woo, J.-H., & Malkan, M. A. 2011, ApJ, 726, 59
- Cavagnolo, K. W., Donahue, M., Voit, G. M., & Sun, M. 2009, ApJS, 182, 12
- Hogan, M. T., McNamara, B. R., Pulido, F. A., et al. 2017, ApJ, 851, 66
- Li, Y., Bryan, G. L., Ruszkowski, M., et al. 2015, ApJ, 811, 73
- McCourt, M., Sharma, P., Quataert, E., & Parrish, I. J. 2012, mnras, 419, 3319
- McDonald, M., Bayliss, M., Benson, B. A., et al. 2012, Nature, 488, 349
- McDonald, M., Swinbank, M., Edge, A. C., et al. 2014, ApJ, 784, 18
- McDonald, M., McNamara, B. R., Voit, G. M., et al. 2019a, arXiv e-prints, arXiv:1904.08942
- McDonald, M., Allen, S. W., Hlavacek-Larrondo, J., et al. 2019b, ApJ, 870, 85
- O'Sullivan, E., Giacintucci, S., Babul, A., et al. 2012, MNRAS, 424, 2971
- Prasad, D., Sharma, P., & Babul, A. 2015, ApJ, 811, 108
- . 2018, ApJ, 863, 62
- Pulido, F. A., McNamara, B. R., Edge, A. C., et al. 2018, ApJ, 853, 177
- Russell, H. R., McDonald, M., McNamara, B. R., et al. 2017, ApJ, 836, 130

Sharma, P., McCourt, M., Parrish, I. J., & Quataert, E.  
2012a, MNRAS, 427, 1219

Sharma, P., McCourt, M., Quataert, E., & Parrish, I. J.  
2012b, MNRAS, 420, 3174

Stern, J., Fielding, D., Faucher-Giguère, C.-A., & Quataert,  
E. 2019, arXiv e-prints, arXiv:1906.07737

Ueda, S., Hayashida, K., Anabuki, N., et al. 2013, ApJ,  
778, 33

Voit, G. M., Bryan, G. L., O'Shea, B. W., & Donahue, M.  
2015a, ApJl, 808, L30

Voit, G. M., Donahue, M., Bryan, G. L., & McDonald, M.  
2015b, Nature, 519, 203